

Forward low-mass enhancement in $p\bar{p}$ seen in reactions in $\pi^-d \rightarrow (n_s)p\bar{p}n$ and $\pi^-d \rightarrow (p_s)p\bar{p}\pi^-$

A. E. Kreymer,* P. Bonamy,[†] B. Brabson, and H. Paik[‡]
Indiana University, Bloomington, Indiana 47405

N. Baggett,[§] C. Baglin,^{||} E. C. Fowler, and D. Hood[¶]
Purdue University, Lafayette, Indiana 47905

T. Fieguth
Stanford Linear Accelerator Center, Stanford, California 94305

M. S. Alam, S. E. Jones,** J. S. Poucher, A. H. Rogers,^{††} and S. Stone^{‡‡}
Vanderbilt University, Nashville, Tennessee 37235
(Received 25 February 1980)

A study of π^-d interactions at 13.2 GeV/c has been performed using the SLAC 2-m streamer chamber with a forward-proton trigger/spectrometer. In this paper, we discuss baryon-antibaryon final states where a forward produced $p\bar{p}$ enhancement is seen near 2.1 GeV in both $p\bar{p}n$ and $p\bar{p}\pi^-n$ final states. The measured cross section for $\pi^-d \rightarrow (n_s)p\bar{p}n$ is $7.6 \pm 1.3 \mu\text{b}$ and for $\pi^-d \rightarrow (p_s)p\bar{p}\pi^-n$ is $6.6 \pm 1.1 \mu\text{b}$ in this experiment.

I. INTRODUCTION

The reaction

$$\pi^-d \rightarrow (p_s)X^-p_{\text{forward}} \quad (1)$$

has been studied using the SLAC 2-m streamer chamber with a forward proton spectrometer in a search for charge -2 manifestly exotic meson states. Results of this work have been reported in a previous paper¹; no statistically significant evidence for new X^- or X^{--} states was found. In this paper we present data on additional features of reactions containing a forward high-momentum proton. In particular, we report on the two reactions $\pi^-d \rightarrow (n_s)p_{\text{fwd}}\bar{p}n$ and $\pi^-d \rightarrow (p_s)p_{\text{fwd}}\bar{p}\pi^-$.

Phase-shift analyses of differential-cross-section and polarization data from the reactions $p\bar{p} \rightarrow \pi^+\pi^-$ and $p\bar{p} \rightarrow K^+K^-$ have shown evidence for a series of rather broad higher-spin resonances in the $p\bar{p}$ system.^{2,3} Also, a partial-wave analysis of the $p\bar{p}$ system, produced in the reaction $\pi^-p \rightarrow p\bar{p}n$ at 18 GeV/c, gives evidence for resonant structure⁴ in the $p\bar{p}$ mass range between 2.0 and 2.8 GeV. The present experiment is sensitive only to highly peripheral $p\bar{p}$ production, where the observed forward proton has at least half the beam momentum and falls into the approximate laboratory angular range of $\pm 2.6^\circ$ vertically and $\pm 4.8^\circ$ horizontally. Under these conditions we observe an enhancement in the $p\bar{p}$ mass spectrum with a mass $M = 2.08 \pm 0.01$ GeV and a width of $\Gamma = 0.11 \pm 0.02$ GeV in the reaction $\pi^-d \rightarrow (n_s)p_{\text{fwd}}\bar{p}n$.⁵ Also, a similar enhancement with $M = 2.09 \pm 0.02$ GeV and $\Gamma = 0.17 \pm 0.05$ GeV is seen in the reaction $\pi^-d \rightarrow (p_s)p_{\text{fwd}}\bar{p}\Delta(1232) \rightarrow (p_s)p_{\text{fwd}}\bar{p}\pi^-n$. These enhancements may be compared to the spin $J = 3^-$

resonance at $M = 2.15$ GeV, $\Gamma = 0.20$ GeV from Ref. 2, or to the $J = 3^-$ resonance at $M = 2.11$ GeV, $\Gamma = 0.21$ GeV from Ref. 3, or to the spin $J = 3^-$ resonance at $M = 2.11$ GeV, $\Gamma = 0.19$ GeV from Ref. 4.

Since this experiment is described in detail elsewhere,^{1,5} we mention only those details germane to the present analysis. A 60-cm-long deuterium target was embedded in the SLAC 2-m streamer chamber. Downstream, a proton spectrometer utilized a pair of counter hodoscopes, large aperture magnet, and pressurized gas threshold Čerenkov counter to identify forward protons with greater than half the π^- beam momentum. The streamer chamber itself provided essentially 4π solid angle charged-particle detection around the target. Background processes such as $K_{\text{fwd}}^+K^-n$ are effectively removed from the trigger by the Čerenkov counter.⁶ In addition, the momentum of the forward proton was well measured giving good missing-mass resolution for identification of final states with an unobserved neutron. Sixteen planes of wire spark chambers in the spectrometer provided 0.6% momentum resolution at 11 GeV/c. The corresponding missing-mass resolution at the neutron mass was approximately 0.20 GeV².

Section II of this paper presents our data for the reaction $\pi^-d \rightarrow (n_s)p_{\text{fwd}}\bar{p}n$ while Sec. III covers the reaction $\pi^-d \rightarrow (p_s)p_{\text{fwd}}\bar{p}\pi^-n$. Section IV discusses possible interpretations of our results.

II. THE REACTION $\pi^-d \rightarrow (n_s)p_{\text{fwd}}\bar{p}n$

Spark-chamber experiments^{4,7} have observed peripherally produced baryon-antibaryon pairs

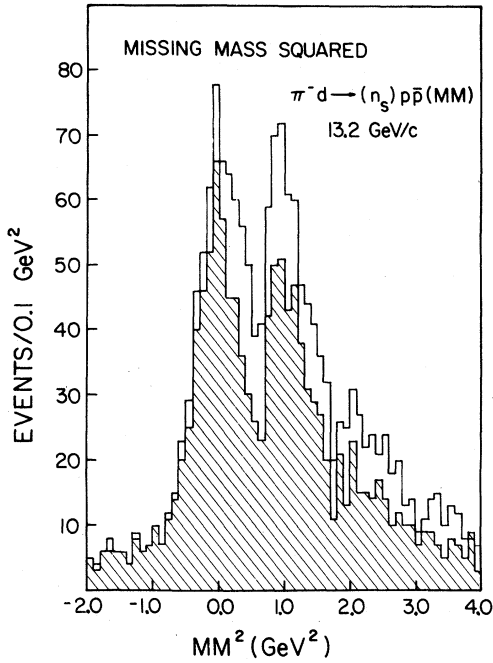


FIG. 1. Missing mass squared (MM^2) from all two-charged-particle events interpreted as $\pi^- d \rightarrow (n_s) p\bar{p} MM$. The cross-hatched histogram has events removed where the charged tracks interpreted as $p\pi^-$ have an effective mass in the N^* interval $1.450 < M(p\pi^-) < 1.750$ GeV.

in the reaction

$$\pi^- p \rightarrow p\bar{p}n. \quad (2)$$

Evidence for this final state in this experiment is seen in Fig. 1. A distinct neutron mass peak appears in the histogram of missing mass squared (MM^2) off of the two charged tracks in two-pronged events. Approximately 145 events appear above

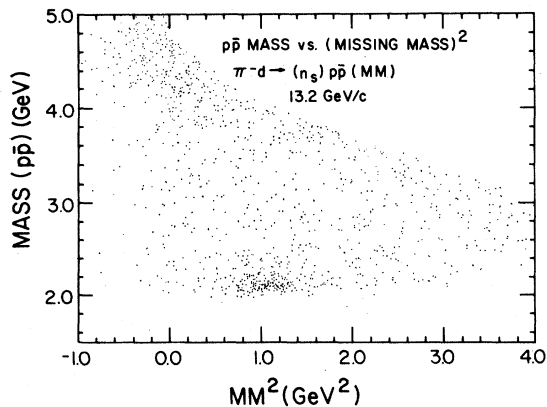


FIG. 2. Scatter plot of two-charged-track events with N^* events [$1.450 < M(p\pi^-) < 1.750$ GeV] removed. The $p\bar{p}$ invariant mass versus the MM^2 is plotted for the reaction $\pi^- d \rightarrow (n_s) p\bar{p} MM$.

a smooth background in the neutron region ($0.7 < MM^2 < 1.3$ GeV²) corresponding to a cross section of 7.6 ± 1.3 μ b. (This is to be compared with 6.5 ± 0.9 μ b at 9.8 GeV/c from Ref. 4.) The large peak near zero MM^2 in this plot results from misidentification of the final states $p_{\text{fwd}}\pi^-(m\pi^0)$, $m = 1, 2, \dots$. Part of this multipion background is identified by a strong N^* enhancement observed in the $p_{\text{fwd}}\pi^-$ system.⁵ Thus, N^* events [$1.45 < M(p_{\text{fwd}}\pi^-) < 1.75$ GeV] are removed, leaving the events shown in Fig. 1, in the cross-hatched histogram. For these events, a scatter plot, Fig. 2, of the mass of the proton-antiproton versus the missing mass squared off of the proton-antiproton shows a strong concentration of events in the neutron band, with a corresponding $p\bar{p}$ mass near 2.1 GeV.

We examine this concentration further by considering those events in the neutron region ($0.7 < MM^2 < 1.3$ GeV²). The background outside this zone is seen as a fairly flat distribution of events in Fig. 2. An interpolation of these events in the "wings" of the scatter plot on either side of the neutron region is subtracted from the events in the neutron band. Then the remaining event distribution is corrected for the geometric acceptance of the apparatus. Figure 3 shows the acceptance-

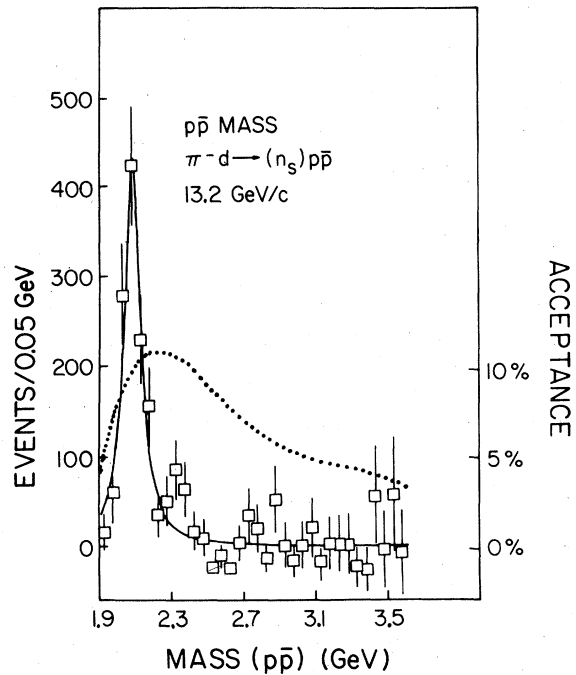


FIG. 3. Acceptance-corrected $p\bar{p}$ mass for two-charged-track events with $0.7 < MM^2 < 1.3$ GeV². The smooth curve is the Breit-Wigner fit described in the text. The dotted curve is the experimental acceptance using the scale on the right.

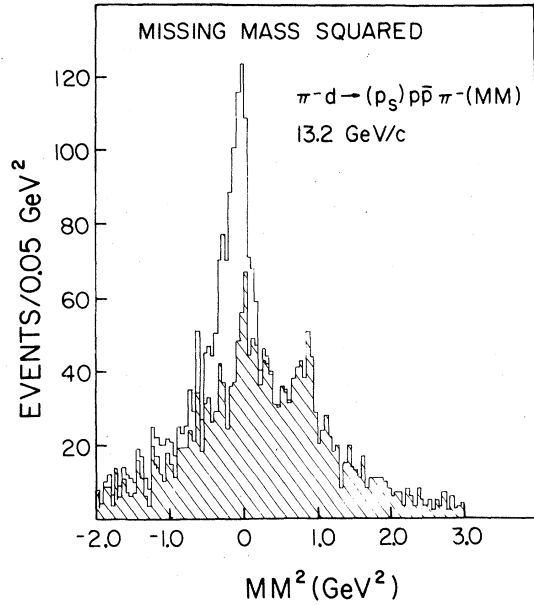


FIG. 4. Missing mass squared (MM^2) for all three-charged-particle events interpreted as $\pi^- d \rightarrow (p_s) p \bar{p} \pi^- (MM)$. The cross-hatched histogram has events removed, where the charged tracks interpreted as $p \pi^- \pi^- (MM)$ have a missing mass squared in the π^0 interval $-0.2 \leq MM^2 \leq 0.45 \text{ GeV}^2$.

corrected events in the neutron band as a function of the $p\bar{p}$ mass. The smooth curve represents an attempt to fit the observed low-mass enhancement to a simple Breit-Wigner distribution. The parameters of the fit are $M = 2.08 \pm 0.01 \text{ GeV}$, $\Gamma = 0.11 \pm 0.02 \text{ GeV}$ with $\chi^2/DF = 0.82$. Our geometric acceptance for a forward produced ($e^{3\nu}$) $p\bar{p}$ system is shown as a dotted line on Fig. 3. Its maximum value is 10.5%.

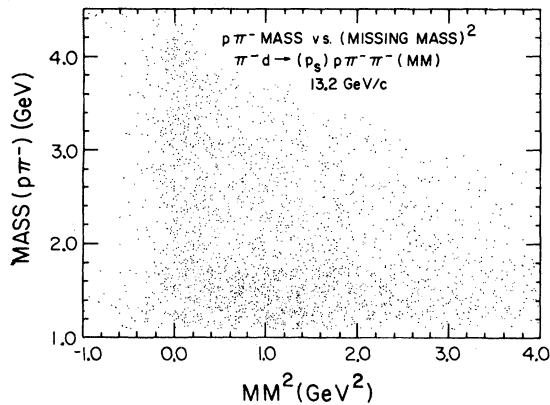


FIG. 5. Scatter plot of all three-charged-track events where the reaction is taken to be $\pi^- d \rightarrow (p_s) p \pi^- \pi^- (MM)$. Two combinations of the invariant mass of $p\pi^-$ are plotted against MM^2 .

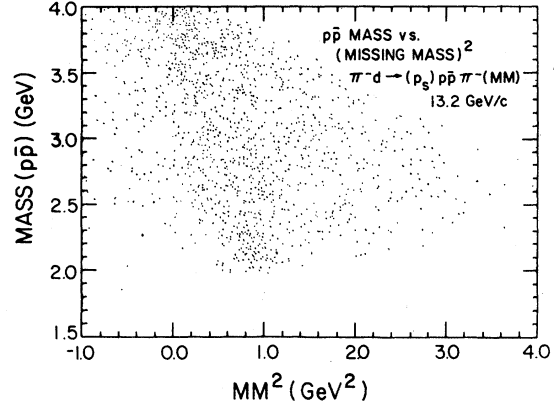


FIG. 6. Scatter plot of three-charged-track events interpreted as $\pi^- d \rightarrow (p_s) p \bar{p} \pi^- (MM)$. Two combinations per event of $p\bar{p}$ invariant mass are plotted against MM^2 .

III. THE REACTION $\pi^- d \rightarrow (p_s) p_{fwd} \bar{p} n \pi^-$

Here we consider the single-constraint reaction

$$\pi^- d \rightarrow (p_s) p_{fwd} \bar{p} n \pi^- \quad (3)$$

Since this channel involves a missing neutron as well as an unseen spectator proton, it is difficult to distinguish from such processes as $\pi^- d \rightarrow (p_s) p_{fwd} \pi^- \pi^- \pi^0$. In an attempt to identify events from reaction (3), measured three-prong events are interpreted as $p_{fwd} \bar{p} \pi^- MM$ and the missing-mass-squared distribution is plotted in Fig. 4. Drawing a smooth curve through the bins near the neutron mass squared we estimate that 120 events come from reaction (3). Interpreting this neutron peak as events of the type $\pi^- d \rightarrow (p_s) (p_f \bar{p}) \pi^- n$ where the $p_f \bar{p}$ system is peripherally produced ($e^{3\nu}$), we calculate an average geometric acceptance of 10% and a corresponding cross section of $6.6 \pm 1.1 \mu\text{b}$.

To isolate the $p\bar{p}$ events from multiple-pion background, we first remove those events of the form $\pi^- d \rightarrow (p_s) p_{fwd} \pi^- \pi^- \pi^0$. Figure 5 shows all three-pronged events interpreted as $p_{fwd} \pi^- \pi^- (MM)$ where MM^2 is plotted against both $p_{fwd} \pi^-$ combinations. The " π^0 " band corresponding to $(-0.2 < MM^2 < 0.45 \text{ GeV}^2)$ is removed, leaving the events in the cross-hatched histogram of Fig. 4. The neutron signal is not appreciably affected by the removal of these events.

Figure 6 shows the remaining events interpreted as $\pi^- d \rightarrow (p_s) p_{fwd} \bar{p} \pi^- (MM)$ where the $p\bar{p}$ invariant mass is plotted against the missing mass squared. As in the $p_{fwd} \bar{p} n$ final state, a concentration of events is seen at the MM^2 of the neutron associated with a low-mass (2.1 GeV) $p\bar{p}$ system. At this point it is interesting to see if the low-mass $p\bar{p}$

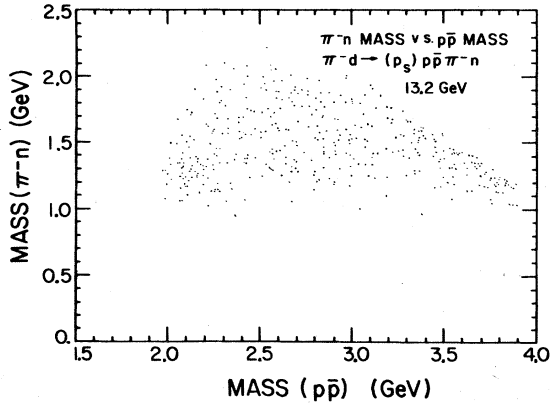


FIG. 7. Scatter plot of those three-charged-track events making a one-constraint fit to the reaction $\pi^- d \rightarrow (\psi_s) p \bar{p} \pi^- n$ with a confidence level greater than 10%. The $\pi^- n$ invariant mass is plotted against the $p \bar{p}$ invariant mass.

enhancement is associated with any particular $\pi^- n$ configuration. A scatter plot (Fig. 7) is made of all events giving a one-constraint fit to the reaction $\pi^- d \rightarrow (\psi_s) p \bar{p} \pi^- n$ with a confidence level greater than 10%. The $p \bar{p}$ mass is plotted against the $\pi^- n$ mass. A cluster of events occurs at the $\pi^- n$ mass near the $\Delta^-(1232)$ together with the low-mass $p \bar{p}$ system near 2.1 GeV. Figure 8 shows the 1-constraint-fit events with $M(\pi^- n) < 1.450$ GeV. The band of events with $1.45 < M(\pi^- n) < 1.80$ GeV has been used to estimate the distribution of events where the $\pi^- n$ system does not resonate. Figure 8 shows the data with this non-resonant background subtracted, and corrected for geometric acceptance. A simple Breit-Wigner fit gives the smooth curve with parameters $M = 2.09 \pm 0.02$ GeV, $\Gamma = 0.17 \pm 0.05$ GeV.

IV. DISCUSSION

π^- -meson exchange provides a consistent picture of forward produced $p \bar{p}$ with a backward neutron.⁴ Let us assume for the moment that pion exchange also dominates the process $\pi^- d \rightarrow (\psi_s) p \bar{p} \Delta^-$ seen in this experiment. The three reactions $\pi^- n \rightarrow p \bar{p} \Delta^- \rightarrow p \bar{p} \pi^- n$, $\pi^- p \rightarrow p \bar{p} \Delta^0 \rightarrow p \bar{p} p \pi^-$, and $\pi^- p \rightarrow p \bar{p} \Delta^0 \rightarrow p \bar{p} n \pi^0$ are related by the usual Clebsch-Gordon coefficients giving an expected cross-section ratio of 9:1:2 for the three reactions, respectively. Since our experiment has roughly the same acceptance for all three processes, it is appropriate to ask whether we would expect to see a $p \bar{p}$ signal in all three channels. We see a $4.2 \mu\text{b}$ (55 events) signal in $p \bar{p} \Delta^-$. This predicts twelve events of $p \bar{p} \Delta^0 \rightarrow p \bar{p} \pi^- n$ and six events of $p \bar{p} \Delta^0 \rightarrow p \bar{p} p \pi^-$. In both cases these numbers are consistent with the event levels observed.⁵ The results from this experi-

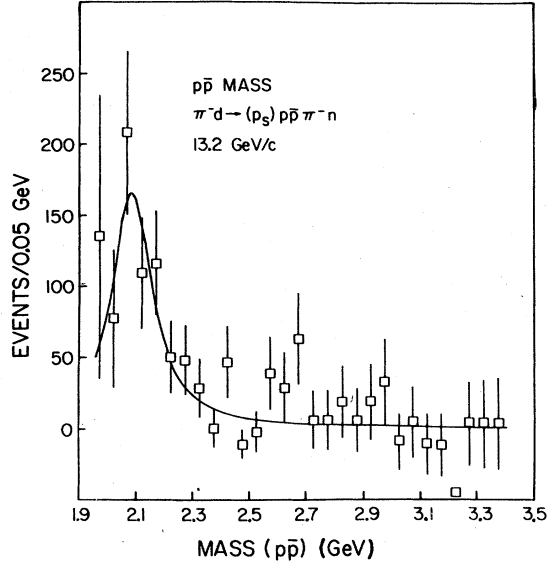


FIG. 8. Acceptance-corrected $p \bar{p}$ invariant mass for three-charged-track events with $1.0 < M(\pi^- n) < 1.45$ GeV. All events in this histogram make a one-constraint fit to $\pi^- d \rightarrow (\psi_s) p \bar{p} \pi^- n$. The smooth curve is the Breit-Wigner fit described in the text.

ment are, therefore, consistent with a pion-exchange picture for the process $\pi^- n \rightarrow p \bar{p} \Delta^-$.

We mention here an alternative explanation for the $p \bar{p}$ enhancements seen in $p \bar{p} n$ and $p \bar{p} \Delta^-$. In a recent paper⁸ Jaffe suggests that the production of narrow baryonium states in meson-baryon scattering should take place in the forward direction mediated by four-quark $qq\bar{q}\bar{q}$ exotic exchange. He uses color arguments pointing out that pairs of quarks in color-sextet states (6- $\bar{6}$ baryonium or mock baryonium) will have inhibited decay into a baryon-antibaryon final state where quark pairs are in color-triplet configurations. The quark-line diagram of this mechanism is shown in Fig. 9.

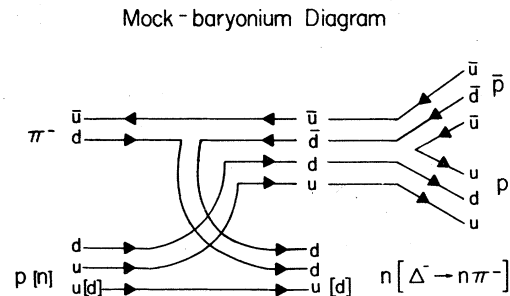


FIG. 9. Exotic-meson-exchange diagram for the production of a forward four-quark system (see Ref. 9) in the reaction $\pi^- p \rightarrow p \bar{p} n$. An alternative quark-line assignment in parentheses corresponds to the reaction $\pi^- n \rightarrow p \bar{p} \Delta^- \rightarrow p \bar{p} \pi^- n$.

Thus, the $p\bar{p}$ forward enhancement in the two reactions $\pi^+p \rightarrow p\bar{p}n$ and $\pi^-n \rightarrow p\bar{p}\Delta^-$ can apparently be described by this exotic-exchange, color-mixing mechanism. We mention two difficulties with this interpretation. First, Jaffe predicts that this exotic mass will be produced forward with a mass near threshold. For example, he suggested looking for a forward-produced (Δ^+p^-) state near 2200 MeV. The enhancement in $p\bar{p}$ seen here is 0.2 GeV above threshold. Second, mock-baryonium states are predicted to have a considerably narrower width than the 0.1 GeV seen here.

The angular momentum barrier between the quark pair and the antiquark pair, used to explain the suppression of mesonic decays of four-quark objects, leads one to expect that narrow baryonium would be a high-spin object. In this regard, it is interesting to note that the $p\bar{p} \rightarrow \pi\pi$ phase-shift results^{1,2} give a rather high-spin assignment of $J=3$ for observed structure in the $M=2.2$ GeV region, and spins of 4 and 5 at higher masses. Two questions immediately come to mind. First, why are the higher-spin states that are observed at 2.35 GeV ($J=4$) and 2.55 GeV ($J=5$) in partial-wave analyses⁹ not seen in this experiment? Although these phase-shift analyses assign a lower production cross section to these higher-mass states, one would expect to see some indication of their presence. Second, why do higher-statistics experiments at surrounding energies and with much wider acceptance not see the same narrow $p\bar{p}$ enhancement at 2.08 GeV? A partial answer to these questions is provided by a closer examination of the effect of our small forward acceptance on the observation of the final state $p\bar{p}n$ studied also in Ref. 4. Our restricted forward proton angular acceptance translates into a rather narrow

Jackson angle interval of acceptance ($1.0 \geq \cos\theta_J \geq 0.2$). If we impose our acceptance upon the Jackson angular distributions from Ref. 9, as a function of $p\bar{p}$ mass, events in the strong forward peak seen in the interval $1.85 \leq M(p\bar{p}) \leq 2.15$ are accepted by our system. This forward peak in the Jackson frame drops away quickly at higher $p\bar{p}$ mass. Thus, our strong enhancement in the 2.1 GeV region from the $p\bar{p}n$ final state is also seen in Ref. 9. The higher-mass structure in Ref. 9 does not contribute substantially to the forward Jackson angles where our experiment is sensitive.

In conclusion, we find a low-mass enhancement in a forward-produced $p\bar{p}$ system both in the reaction $\pi^-d \rightarrow (n_s)p_{fwd}\bar{p}n$ and in the reaction $\pi^-d \rightarrow (p_s)p_{fwd}\bar{p}\Delta^-$. Our observations in both cases are consistent with a single-pion-exchange mechanism. Also, our $\pi^-d \rightarrow (n_s)p_{fwd}\bar{p}n$ data agree with data from the reaction $\pi^+p \rightarrow p_{fwd}\bar{p}n$ measured by other groups.^{4,7,9} Finally, our observation of a low-mass enhancement at $M=2.08$ GeV in the reaction $\pi^-d \rightarrow (p_s)p_{fwd}\bar{p}n$ strongly suggests that a similar mechanism explains both reactions.

ACKNOWLEDGMENTS

We would like to thank R. Mozley and the members of Group D at SLAC who contributed enormously to the successful running of the present experiment. Also, we wish to thank the scanning and measuring staffs at both Indiana and Vanderbilt Universities. In particular, we thank C. Ellis for his contributions to the measurement of film at Indiana University using the precision-encoding and pattern-recognition system (PEPR). The work was supported by the U.S. Department of Energy (Indiana University, Purdue University, and SLAC) and by the National Science Foundation (Vanderbilt University).

*Present address: P. C. Box 500, Fermilab, Batavia, Illinois 60510.

†On leave of absence from C.E.N. Saclay, B. P. No. 2, F-91190, Gif-sur-Yvette, France.

‡Present address: IUPUI, Indianapolis, IN 46205.

§Present address: D.O.E. High Energy Physics, Washington, D. C. 20545.

||On leave of absence from Laboratoire d'Annecy-le-Vieux, B.P. 909, F-74019, Annecy-le-Vieux, France.

¶Present address: David Lipscomb College, Nashville, TN 37203.

**Present address: E.G.&G., Idaho Falls, Idaho 83401.

††Present address: SLAC, Stanford, CA 94305.

‡‡Present address: Newman Laboratory, Cornell University, Ithaca, N. Y. 14853.

¹M. S. Alam *et al.*, Phys. Rev. Lett. **40**, 1685 (1978).

²A. A. Carter *et al.*, Phys. Lett. **67B**, 117 (1977).

³A. Donnachie and P. R. Thomas, Nuovo Cimento **26A**, 317 (1975).

⁴B. Hyams *et al.*, Nucl. Phys. **B73**, 202 (1974).

⁵A. E. Kreymer, Ph.D. thesis, Indiana University, 1979, Report No. IUHEE 30 (unpublished); D. W. Hood, Ph.D. thesis, Purdue University, 1978 (unpublished).

⁶Using the known Čerenkov inefficiency for removing low momentum K^+ 's [see S. E. Jones, Ph.D. thesis Vanderbilt University, 1978 (unpublished), p. 101] and using known forward K^+ production cross sections, we estimate a two-event K^+K^-n contamination in the $p\bar{p}n$ sample. Also, as a check against a large K^+K^-n contamination, we see no evidence for known structure in the K^+K^-n channel when K interpretations were given to the charged tracks.

⁷R. S. Dulude and J. A. Gaidos, Nucl. Phys. B91, 77 (1975).

⁸R. L. Jaffe, Univ. of Oxford, Report No. 16/79 (unpublished). Jaffe discusses this diagram with slightly

different quark-line assignments leading to the reactions $\pi^-p \rightarrow (\Delta^{++}\bar{p})_{\text{fwd}}\Delta^-$ and $\pi^-p \rightarrow (p\bar{\Delta}^0)_{\text{fwd}}\Delta^-$.

⁹G. Grayer *et al.*, Phys. Lett. 39B, 563 (1972); M. Rozanska *et al.*, Nucl. Phys. B162, 505 (1980).